Progress in Oceanography xxx (2014) xxx–xxx

Contents lists available at ScienceDirect

Progress in Oceanography

journal homepage: www.elsevier.com/locate/pocean

Upwind dynamic soaring of albatrosses and UAVs

Philip L. Richardson *

Department of Physical Oceanography MS#29, Woods Hole Oceanographic Institution, 360 Woods Hole Road, Woods Hole, MA 02543, USA

ARTICLE INFO

Article history:
Received 22 May 2014
Received in revised form 1 November 2014
Accepted 3 November 2014
Available online xxxx

ABSTRACT

Albatrosses have been observed to soar in an upwind direction using what is called here an upwind mode of dynamic soaring. The upwind mode was modeled using the dynamics of a two-layer Rayleigh cycle in which the lower layer has zero velocity and the upper layer has a uniform wind speed of *W*. The upwind mode consists of a climb across the wind-shear layer headed upwind, a 90° turn and descent across the wind-shear layer perpendicular to the wind, followed by a 90° turn into the wind. The increase of airspeed gained from crossing the wind-shear layer headed upwind was balanced by the decrease of airspeed caused by drag. Results show that a wandering albatross can soar over the ocean in an upwind direction at a mean speed of 8.4 m/s in a 3.6 m/s wind, which is the minimum wind speed necessary for sustained dynamic soaring. A main result is that albatrosses can soar upwind much faster than the wind speed. Furthermore, albatrosses were found to be able to increase upwind speeds in winds greater than 3.6 m/s, reaching an upwind speed of 12.1 m/s in a wind speed of 7 m/s (for example).

The upwind dynamic soaring mode of a possible robotic albatross UAV (Unmanned Aerial Vehicle) was modeled using a Rayleigh cycle and characteristics of a high-performance glider. Maximum possible airspeeds are equal to approximately 9.5 times the wind speed of the upper layer. In a wind of 10 m/s, the maximum possible upwind (56 m/s) and across-wind (61 m/s) components of UAV velocity over the ocean result in a diagonal upwind velocity of 83 m/s. In sufficient wind, a UAV could, in principle, use fast diagonal speeds to rapidly survey large areas of the ocean surface and the marine boundary layer. In practice, the maximum speeds of a UAV soaring over the ocean could be significantly less than these predictions. Some limitations to achieving fast travel velocities over the ocean are discussed and suggestions are made for further studies to test the concept of a robotic albatross.

Introduction

On a research cruise to the South Atlantic I watched with amazement as a wandering albatross soared upwind parallel to our ship, which was steaming upwind at 6 m/s (12 knots) into an estimated 7 m/s head wind. The bird came from leeward of the ship and caught up with us, indicating that it was soaring significantly faster than our 6 m/s speed. It remained soaring upwind at least 100 m across-wind from the ship, which suggested the bird was little influenced by the ship's disturbance of the wind field. At first thought, it seemed almost impossible that an albatross could soar upwind without flapping its wings with a mean velocity through the air faster than 13 m/s and significantly faster than the 7 m/s wind. More observations of albatrosses soaring upwind made by myself and others (Pennycuick, 1982; Wakefield et al., 2009) and further reflection suggested that such upwind soaring is made possible primarily by using dynamic soaring to exploit wind shear, probably supplemented by updrafts over waves.

The term dynamic soaring refers to the extraction of energy from the gradient of wind velocity. In dynamic soaring an albatross typically climbs across the wind-shear layer while headed upwind, turns to head downwind, descends down across the wind-shear layer, and then turns upwind again (Baines, 1889; Idrac, 1925; Pennycuick, 2002). An albatross usually executes these two turns in an S-shaped maneuver while soaring across-wind, which is the preferred direction for albatross soaring (Alerstam et al., 1993; Wakefield et al., 2009). Both crossings of the wind-shear layer and the turn downwind can provide energy for sustained or energy-neutral soaring, but the apparent source of energy depends on the reference frame. In the two-layer model discussed in this paper, all of the increase of airspeed and airspeed kinetic energy comes from the bird's climb and descent across the wind-shear layer. All of the increase of ground speed and ground speed kinetic energy comes from the banked turn in the upper layer as the bird changes direction from headed upwind to downwind. There is an equal gain of energy in the two reference frames.

Despite many studies of dynamic soaring there is still uncertainty about how fast an albatross (or a UAV) can soar upwind using dynamic soaring. The uncertainty is caused in part by the

* Tel.: +1 508 289 2546 (W), +1 508 540 2648 (H); fax: +1 508 457 2163.
E-mail address: prichardson@whoi.edu

http://dx.doi.org/10.1016/j.pocean.2014.11.002
0079-6611/

relatively few observations of albatrosses soaring into a headwind and in part by the slow upwind velocity predicted by models of dynamic soaring that use an average wind profile above a flat ocean surface. The relatively few observations of upwind flight are probably explained by the fact that more work is required to soar upwind than in other directions. Evidence for this is provided by Weimerskirch et al. (2000), who documented that soaring upwind is associated with faster heart rates of wandering albatrosses compared to across-wind and down-wind flight in which heart rates are sometimes close to basal levels. This increased heart rate is probably not caused by wing flapping because Pennycuick (1982) observed that wandering albatrosses soar directly into the wind without flapping their wings (at wind speeds greater than 3 m/s). My own observations of wandering albatrosses revealed the same thing. This suggests that wing flapping of wandering albatrosses is not required for soaring upwind (or in any other direction) at wind speeds above around 3 m/s and that upwind flight speed is not augmented by wing flapping.

There are definite benefits for an albatross to being able to soar fast upwind such as being able to rapidly travel to a good upwind fishing ground, being able to return and feed a hungry chick after being caught downwind in a wind shift, and being able to keep up with a ship and scavenge discarded food scraps or discarded fishing bycatch. This last potential benefit was probably why the albatross was shadowing our ship, which had numerous spools of wire and other mooring gear on the fantail and thus resembled a commercial fishing vessel. A clear benefit for a UAV to being able to soar fast upwind is the ability to fly rapidly in any direction relative to the wind as part of survey missions.

The purpose of this paper is to explain how an albatross can fly fast upwind by using a particular form of dynamic soaring that is somewhat different from the usual across-wind dynamic soaring maneuver. In particular a bird is able to achieve fast upwind flight by using a series of 90° turns, starting with a climb across the shear layer headed upwind banked to the right (for example), then a descent across the shear layer headed across wind, and switching to a banked turn to the left toward the wind direction again. The albatross shadowing our research ship was doing this maneuver, starting headed across wind in a wave trough, turning upwind and climbing over the top of a wave, then turning back across wind and diving down into another wave trough.

The goal of this paper is to explore the upwind mode of travel velocity by using the Rayleigh cycle model to predict upwind travel velocities of a wandering albatross and a robotic-albatross type UAV (Unmanned Aerial Vehicle). Part of the motivation for this study is to investigate the possible development of a robotic albatross UAV that could soar over the ocean using dynamic soaring like an albatross but faster because of superior strength and better aerodynamic performance. Possibly, such a UAV could be used in environmental monitoring, search and rescue, and surveillance. In order to evaluate how effectively a UAV could survey the ocean, it is necessary to establish typical upwind and across-wind soaring abilities. The UAV soaring was modeled on the observed soaring flight of a wandering albatross (Diomedea exulans).

Review of previous studies of upwind dynamic soaring

Albatross GPS tracking

Wakefield et al. (2009) analyzed a large amount of GPS tracking data of albatrosses and found a linear relationship between their ground speed and the component of wind speed (at a height of 5 m) in the direction of flight. For example, the ground speed of a wandering albatross was found to equal an average 11.9 (±0.6) m/s plus 0.59 (±0.06) times wind-speed component in the direction of ground velocity (their Fig. 2 and Table 3). These results suggest that albatrosses generally fly with an average 12 m/s travel velocity through the air even in relatively fast winds of 10 m/s and in the corresponding large wind shears. An implication is that the birds control the amount of energy in dynamic soaring in order to maintain a nearly constant average airspeed. However, there is significant scatter about the mean linear relationship and in plots of ground velocity plotted relative to the wind direction, which were kindly provided by Wakefield (personal communication). These indicate that albatrosses can occasionally soar upwind considerable faster than the average 11.9 m/s plus 0.6 times wind component in the direction of flight. Some upwind ground speeds of around 10–15 m/s were measured corresponding to wind speeds of 5–10 m/s. These GPS data indicate that at times albatrosses are quite capable of exploiting moderately fast wind speeds in order to soar significantly faster upwind through the air than the typical cruise airspeed.

Previous simulations of upwind dynamic soaring

Lissaman (2005), Richardson (2011), and Bower (2012), discussed dynamic soaring using a two-layer, wind-step model, although Bower did not simulate soaring trajectories using the wind step and Lissaman only simulated across-wind flight. Upwind flight was simulated by Richardson (2011) by assuming that the across-wind soaring mode could be tilted in upwind directions, but this required faster wind speeds than for across-wind flight (assuming an average albatross airspeed of 16 m/s). A maximum upwind speed of 6.2 m/s was found for a diagonal upwind velocity of 7.1 m/s in a direction of 30 degrees relative to the wind direction and in a wind speed of 6.8 m/s. The 6.2 m/s upwind speed was large enough to explain my observations of the albatross soaring at the ship speed (6 m/s) but not the observations of the albatross catching up to the ship from leeward, nor the faster upwind GPS tracking speeds shown by Wakefield et al. (2009). This suggests that the tilted across-wind model is not sufficient to explain the observations and that albatrosses might be able to exploit faster wind speeds to fly at faster airspeeds.

Several aerodynamic models of dynamic soaring assume an exponential or a logarithmic mean wind profile over a flat ocean (no waves). This assumption of a flat ocean implies that these models are most appropriate for dynamic soaring in regions without waves such as harbors, where albatrosses have been observed to exploit dynamic soaring. Deittert et al. (2009) modeled a UAV and obtained modest upwind travel velocities reaching around 2–6 m/s in an exponential wind profile with wind speeds of 8–20 m/s referenced to a height of 20 m. These upwind velocities (2–6 m/s) are much slower than some of the upwind travel velocities of albatrosses measured by GPS (Wakefield et al., 2009) despite the model UAV having a larger maximum lift/drag (33.4) than that of wandering albatrosses (21.2). There are at least two explanations for the relatively slow simulated upwind UAV speeds. The first is that most (~70%) of the increase of wind speed above the ocean in the 20 m exponential wind layer occurs in the first 1.5 m above the surface. Thus most of the increase of wind speed in the profile was missed by the UAV because of its banked wings plus an additional distance above the ocean surface for safety. The second major difference is that the UAV always remained in the contrary winds above the surface and thus had a large downwind leeway (advection by the wind). Deittert et al. showed a detailed plot of a direct upwind snaking mode of flight with heights between approximately 1–25 m in a wind with a speed of 12 m/s at 20 m. The leeway is around 11 m/s, which appears to limit the maximum upwind travel velocity to around 6 m/s.

Barnes (2004) simulated the direct upwind snaking mode of a UAV (maximum lift/drag ~27) using an exponential wind profile

Please cite this article in press as: Richardson, P.L. Upwind dynamic soaring of albatrosses and UAVs. Prog. Oceanogr. (2014), http://dx.doi.org/10.1016/j.pocean.2014.11.002

with a wind speed of 7 m/s at a height of 20 m. His predicted UAV upwind travel velocity was 3.6 m/s. Bower (2012) modeled a UAV (maximum lift/drag = 25) dynamic soaring in a logarithmic wind profile. He plotted a speed polar for winds of 8–20 m/s referenced to a height of 20 m and found a maximum upwind UAV speed of 2.5 m/s (his Fig. 4.4).

These relatively slow upwind travel velocities obtained by Barnes (2004), Deittert et al. (2009), and Bower (2012), emphasize that in order to fly fast upwind it is important to exploit the full wind-shear layer located just above wave crests and to remain in the slow winds located downwind of wave crests for part of the flight. Albatross flight typically includes both of these features—flight in wave troughs and climbs upwind across the main wind-shear layer—similar to the gust-soaring technique proposed by Pennycuick (2002).

Rayleigh cycle model of dynamic soaring

Lord Rayleigh (1883) was the first to describe how a bird could use the vertical gradient of the wind velocity to obtain energy for sustained dynamic soaring, although he did not call it that. He envisioned a two-layer model with different wind speeds (W) in the two layers, the speeds differing by an amount indicated by ΔW. He described how a circling bird could gain airspeed equal to ΔW by climbing headed upwind across the boundary between layers and gaining another ΔW by descending headed downwind across the boundary, a total gain of $2\Delta W$ in a circle (Fig. 1). If ΔW is sufficiently large, then enough energy could be obtained by this maneuver to sustain soaring. This maneuver has become known as the Rayleigh cycle.

In order to develop a (fairly) simple dynamic model of albatross dynamic soaring Richardson (2011) balanced the airspeed gain in the Rayleigh cycle with the loss of energy due to the drag of the air acting on the bird as described by Lissaman (2005). The model is referred to as the Raleigh cycle model and is used in this paper. Drag was modeled with a quadratic drag law in which the drag coefficient is proportional to the lift coefficient squared. Two homogenous layers were assumed, a lower layer of zero wind speed and upper layer of wind speed W. A thin wind-shear layer is sandwiched between the upper and lower layers. The zero wind speed in the lower layer represents the region of low wind speeds located in wave troughs. The wind in the upper layer represents the fast wind blowing above wave crests. This model agrees with the concept of an albatross gust soaring proposed by Pennycuick (2002) in which a wind gust is encountered when a bird pulls up from the low-wind region in a wave trough into the faster wind (the gust) located just above a wave crest.

The essential assumptions in the Rayleigh cycle model are that (1) the bird soars in nearly circular loops along a plane tilted upward into the wind, (2) the plane crosses the wind-shear layer at a small angle with respect to the horizon so that vertical motions can be ignored, (3) the average airspeed and average glide ratio can be used to represent flight in the circle, and (4) conservation of energy in each layer requires a balance between the sudden increase of airspeed (and kinetic energy) caused by crossing the shear layer and the gradual loss of airspeed due to drag over each half loop, resulting in energy neutral soaring (see Appendix A for a more complete description of the model.)

Discussion of the assumed zero velocity in the lower layer

An important assumption is zero wind velocity in the lower layer, which represents the low speed region in wave troughs. An issue that needs to be considered is whether or not this could lead to a significant underestimate of albatross leeway. A fast wind flowing over a relatively slow wave often causes a lee eddy, which is a region of closed streamlines centered about the critical layer and synchronous with the wave (Sullivan et al., 2000). Sometimes a lee eddy is known as a cat's eye for its distinctive pattern of streamlines. The region of closed streamlines in the lee eddy deflects the outer mean streamlines away from the wave surface creating a region of updraft over the eddy. Hristov et al. (2003) also show observations and model calculations of wind-wave interactions and induced lee eddies. The waves modeled by Sullivan et al. (2000) are sinusoidal. Wind waves tend to have sharper crests

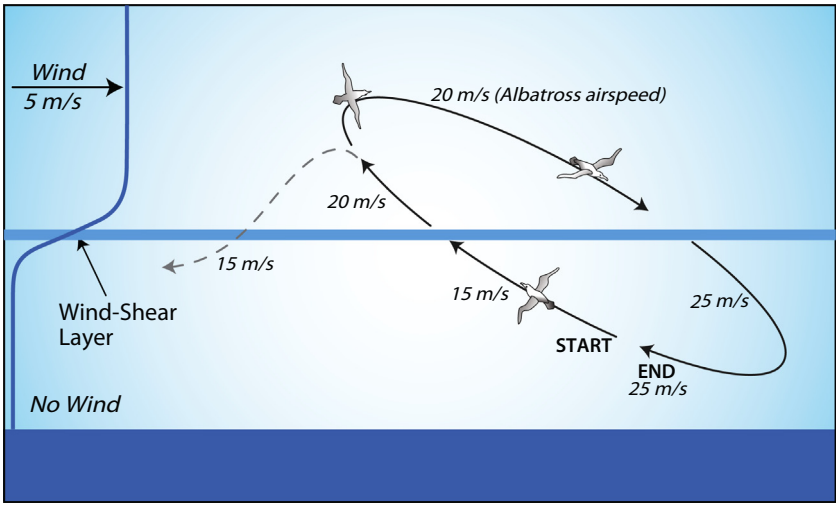

Fig. 1. Idealized example of the airspeeds of a dragless albatross dynamic soaring through a thin wind-shear layer, which is assumed to consist of an increase in wind speed from zero below the layer to 5 m/s above. The zero speed in the lower layer represents the low wind speed located in wave troughs. This schematic is based on the written description of Rayleigh (1883) who first suggested that a bird could continuously soar in nearly-circular flight on an inclined plane that crosses a thin wind-shear layer. Starting in the lower layer with an airspeed 15 m/s a bird climbs upwind a short distance vertically across the wind-shear layer, which increases airspeed to 20 m/s. The bird turns and flies downwind with the same airspeed of 20 m/s. During the turn, ground speed increases to 25 m/s in a downwind direction and consists of the bird's 20 m/s airspeed plus (tail) wind speed of 5 m/s. The bird descends downwind a short distance vertically across the wind-shear layer, which increases airspeed to 25 m/s. Flying with an airspeed of 25 m/s the bird turns upwind. Thus, one circle through the wind-shear layer increases airspeed and ground speed from 15 m/s to 25 m/s (two times the 5 m/s wind speed increase across the wind-shear layer). By descending upwind (dashed line) the bird's airspeed would have decreased from 20 m/s back to 15 m/s with no net gain in airspeed. This schematic shows an oblique view of near-circular flight.

Please cite this article in press as: Richardson, P.L. Upwind dynamic soaring of albatrosses and UAVs. Prog. Oceanogr. (2014), http://dx.doi.org/10.1016/j.pocean.2014.11.002

than this and can break in sufficient wind speed. When swift wind blows over a sharp-crested wave or a breaking wave, streamlines can separate from the wave as described by Pennycuick (2002). The resulting lee eddy or separation bubble also contains closed streamlines. Other examples of lee eddies are shown by Hsu et al. (1981), Gent and Taylor (1977), and Reul et al. (1999).

Because the phase speed of wind waves is downwind, a lee eddy in a wave trough would have a net downwind velocity. However, the albatross I observed soaring rapidly upwind was soaring over what looked like a confused sea without a set of uniform wind-driven waves and troughs propagating downwind. Instead, there appeared to be significant cross seas, which included swell waves propagating in from elsewhere at an angle to the wind waves. Both sets of waves, local wind waves and swell waves, were difficult to clearly resolve visually. The point is that the albatross I observed was not just periodically following simple wave troughs in a downwind direction but instead seemed to be picking out a general across-wind path through the confused seas, possibly taking advantage of particular large wave crests and troughs to help do this and to exploit the wind-shear layer. In situations like this where a swell is running at an angle to the wind some wave crests and troughs are tilted into the wind, and that could enable an albatross to periodically follow a wave trough and not necessarily be carried downwind, especially when swell is propagating upwind. For these reasons, I think the assumption of a zero velocity lower layer is not an unreasonable one. Certainly there could be a downwind component of wind in the lower layer, which could lead to increased leeway, but it would be difficult to model without knowing more details about the in situ wind and wave fields and details about how an albatross actually dynamically soars.

One possible way to evaluate the relevance of the assumption of zero velocity in the lower layer is to compare the model leeway with that of tracked albatrosses. The Wakefield et al. (2009) analysis can be interpreted to indicate that the average leeway experienced by wandering albatrosses is given by the slope of the regression line (0.59) times the wind speed at a height of 5 m. The Rayleigh cycle model used here assumes that albatrosses spend approximately equal amounts of time in each layer, which indicates the bird's leeway is equal to 0.50 times the wind speed of the upper layer. If we assume that the wind speed of the upper model layer is represented by the wind speed at 5 m, then the modeled leeway is 0.50 times the wind speed at 5 m. This value (0.50) is 15% smaller than the observed value of 0.59. The implication is that the Rayleigh model leeway under represents true leeway by a relatively small amount (~15%).

In order to investigate this issue further I analyzed a larger data set of wandering albatross tracking data consisting of 831 velocities determined with GPS positions spaced at 15 min. These data, kindly provided by Ewan Wakefield, have a higher temporal resolution than those analyzed earlier by Wakefield et al. (2009). The slope of the regression line through the flight speeds and wind components at a height of 5 m in the direction of flight is 0.50 ± 0.04, where ±0.04 are the 95% confidence limits. These more numerous and higher resolution data indicate that the assumed leeway (0.50 times wind speed) is in close agreement with leeway of wandering albatrosses.

There are uncertainties in this interpretation because the calculated slope depends on the chosen reference height (5 m) of the wind, the leeway encountered by the birds, and any variation of the bird's airspeed associated with variations of wind speed, flight direction relative to the wind, updrafts over waves, etc. The good agreement between the Rayleigh cycle model's simulated upwind velocities and those measured by GPS tracking implies that the simulated leeway is pretty close to real albatross leeway, much closer than models that use mean wind profiles over a flat ocean. For example, combining the 11 m/s leeway estimated for the Deittert et al. (2009) UAV (mentioned above) and the corresponding wind speed reduced to a reference height of 5 m indicates that the leeway would be around 1.2 times the wind speed at 5 m (9.4 m/s), or more than two times larger than the leeway of tracked albatrosses.

Dynamic soaring maneuvers

I have observed albatrosses to fly in three typical dynamic soaring maneuvers. The first is a circling hover mode with a bird's wings banked in the same direction similar to the basic Rayleigh cycle shown schematically in Fig. 1. A minor modification of this is a figure-eight-shaped hover mode in which a bird switches the direction of its banked wings on every other crossing of the shear layer. The second maneuver is an across-wind travel mode, consisting of a series of 180° turns banked successively right then left (say), while the bird is headed on an average course across the wind (Fig. 2). Using this mode, an albatross can soar quite fast perpendicular to the wind velocity. Albatross tracking suggests that this is the usual soaring mode (Alerstam et al., 1993; Wakefield et al., 2009). A third maneuver is an upwind travel mode in which an albatross can soar quite fast in an upwind direction as Idrac (1925) and I have observed (Fig. 2). I believe that this upwind mode better represents how an albatross actually soars upwind and is a more efficient way to do so than the tilted across-wind mode (Richardson, 2011).

Upwind travel mode

In this mode a bird first climbs up across the wind-shear layer headed upwind, banks and turns 90° to the right (say). The bird then descends across the wind-shear layer headed perpendicular to the wind, banks left and turns 90° into the wind again. Using

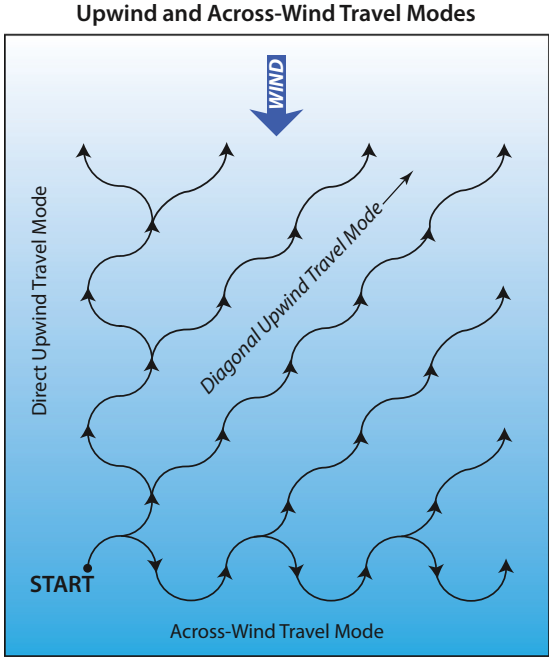

Fig. 2. Schematic examples of upwind and across-wind modes of dynamic soaring created by linking 90° and 180° turns into snaking flight patterns. The 16.0 m/s cruise airspeed of a wandering albatross was used to calculate a 10.2 m/s mean travel velocity through the air in the across-wind and along-wind directions and diagonal travel velocities of 14.4 m/s. Arrow heads are placed at points where the bird crosses the wind-shear layer when headed either upwind or downwind thereby gaining airspeed and kinetic energy.

Please cite this article in press as: Richardson, P.L. Upwind dynamic soaring of albatrosses and UAVs. Prog. Oceanogr. (2014), http://dx.doi.org/10.1016/j.pocean.2014.11.002

a series of 90° turns a bird zig–zags diagonally upwind through the air at an average angle of around 45° relative to the wind direction (Fig. 2). By adjusting the direction of the turns, either to the left or right after an upwind climb, a bird can effectively tack in any direction it chooses including (on average) directly upwind. To soar directly upwind the bird would execute a series of turns, first right then left, after upwind climbs resulting in a series of 180° turns similar to the across-wind mode (Fig. 2). This technique could also be also used for fast down-wind soaring if a bird replaces upwind climbs across the wind-shear layer with downwind descents across the wind-shear layer.

The energy balance in a set of two 90° turns in the diagonal upwind mode is almost exactly the same as in one 180° turn. Airspeed gained in an upwind crossing of the wind-shear layer is reduced by drag during the two 90° turns, which equal the same amount of angular turn as one 180° turn. The main difference is an extra change in banking direction between 90° turns. As long as the bird can change its bank angle rapidly compared to the whole maneuver then the dynamics would be unchanged from the basic circular Rayleigh cycle model. The typical observed period of time for the two 180° turns of the hover mode and the across-wind mode is around 10 s for a wandering albatross, and thus the implied period of two 90° turns would be around 5 s. However, the albatross I observed soaring upwind completed the two 90° turns in around 10 s. (More about this below.)

Numerical example of upwind travel mode

The cruise airspeed, V_c = 16 m/s, of a wandering albatross is its speed at the maximum glide ratio, which is around 21.2 in straight flight (Pennycuick, 2008). Using these values, the observed loop period of 10 s, the aerodynamic equations of motion and the Rayleigh cycle model I found that the minimum wind speed in the upper layer that can support energy-neutral dynamic soaring is 3.6 m/s (Eq. (A4)). This value is in good agreement with the results of numerical simulations using the full aerodynamic equations (Lissaman, 2005, and personal communication; Sachs, 2005; Richardson, 2011). The Raleigh cycle model predicts that the bird's airspeed would be 14.2 m/s just before crossing the shear layer, would increase by 3.6 m/s on crossing the shear layer, and would reach 17.8 m/s just afterward. The 17.8 m/s speed would then be reduced by drag to 14.2 m/s by the end of a 180° turn or two 90° turns. The average bank angle of the maneuver would be around 46° and the average acceleration acting on the bird around 1.4 *g*.

The average across-wind travel velocity through the air of an albatross is equal to the diameter of a 180° semi-circular turn divided by the 5 s to fly it. Thus the across-wind component of soaring flight would be equal to $2V_c/\pi$ = 10.2 m/s, where V_c is the 16 m/s cruise airspeed (Table 1, Fig. 3). In the upwind mode of flight consisting of a series of 90° or 180° turns, the average upwind velocity through the air would also equal 10.2 m/s (assuming the same 5 s to fly 180°), as would the downwind velocity. Diagonal travel velocity at an angle of 45° relative to the wind is the resultant of the across-wind and upwind values and equals 14.4 m/s, almost as fast as the bird's cruise airspeed (16 m/s). The relatively fast diagonal travel velocity is possible because the diagonal series of linked 90° turns more closely approximates a straight course than does a series of linked 180° turns in the across-wind or upwind directions.

Leeway

In all three modes of dynamic soaring maneuvers there is downwind leeway caused by the portion of flight in the upper wind layer. A bird spends approximately half of its time in each layer and thus the average leeway in a maneuver equals around one half of the wind velocity of the upper layer. This leeway value needs to be applied to the bird's mean velocity through the air in order to obtain the bird's travel velocity over the ground. In principle, a bird could extend the upwind flight legs to compensate for leeway. This would make the hover mode more stationary and make the across-wind travel mode perpendicular to the wind. It would require gaining a bit more energy from the wind-shear layer and a slightly faster wind than that without compensating for leeway.

In the upwind mode, the upwind velocity through the air of 10.2 m/s would be countered by leeway of 1.8 m/s (half the wind speed in the upper layer) resulting in an upwind travel velocity over the ground of 8.4 m/s (Table 1, Fig. 3). Correcting for leeway results in a diagonal upwind travel velocity of 13.2 m/s at a direction of around 51° relative to the wind. In a 7 m/s wind the upwind travel velocity would be 6.7 m/s, enough for an albatross to follow our ship but not enough to rapidly catch up from astern.

The diagonal travel velocity over the ground is significantly faster than either the direct upwind or across-wind travel velocities. This suggests that diagonal flight would be the fastest way to travel over the ocean, especially downwind diagonal flight at 15.7 m/s (Table 1, Fig. 3), which is very close to the bird's 16 m/s cruise velocity through the air. An albatross could choose a diagonal flight mode in order to make the fastest passage to feeding grounds or a fast return. An implication is that the fastest way an albatross could search a particular region for food would be to use a diagonal flight pattern.

Across-wind descent

An important detail should be mentioned about the descent across the wind-shear layer when headed perpendicular to the

Table 1
Wandering albatross and UAV travel velocities.

Travel direction	Wandering albatross (V_c = 16 m/s)		UAV (V = 9.5W)	
	Travel velocity through air (m/s)	Travel velocity over ground (m/s)	Travel velocity through air	Travel velocity over ground
Upwind	10.2	8.4	6.1W	5.6W
Diagonal upwind	14.4	13.2 (51°)	8.6W	8.3W (47°)
Downwind	10.2	12.0	6.1W	6.6W
Diagonal downwind	14.4	15.7 (140°)	8.6W	9.0W (137°)
Across-wind	10.2	10.2	6.1W	6.1W

Values of travel velocity (m/s) of a wandering albatross were calculated using its cruise airspeed (V_c) of 16 m/s at the maximum lift/drag ratio of 21.2, a loop period of 10 s, the Rayleigh cycle model, a wind speed of 3.6 m/s (the minimum for dynamic soaring), and a combination of upwind and across-wind soaring modes as shown in Fig. 2. The average bank angle is 46° and average acceleration is 1.4 *g*. The UAV's maximum airspeed was calculated with the Rayleigh cycle model to be 9.5W, where W is the wind speed in the upper layer (Eq. (A10), see text). This relation, UAV airspeed = 9.5W, is a good approximation for wind speeds greater than around 5 m/s. UAV travel velocities were calculated using this airspeed and a combination of soaring modes as shown in Fig. 2. In order to obtain the travel velocity over the ground, values of travel velocity through the air were corrected for leeway, estimated to be one half the wind speed of the upper layer. Values in parentheses are the angles of travel velocity relative to the wind direction, which was assumed to be from zero degrees. Velocity values of a UAV represent the maximum possible using the Rayleigh cycle model and characteristics of a Kinetic 100DP glider. These velocities are probably significantly larger than those obtainable by a UAV soaring over ocean waves.

Please cite this article in press as: Richardson, P.L. Upwind dynamic soaring of albatrosses and UAVs. Prog. Oceanogr. (2014), http://dx.doi.org/10.1016/j.pocean.2014.11.002

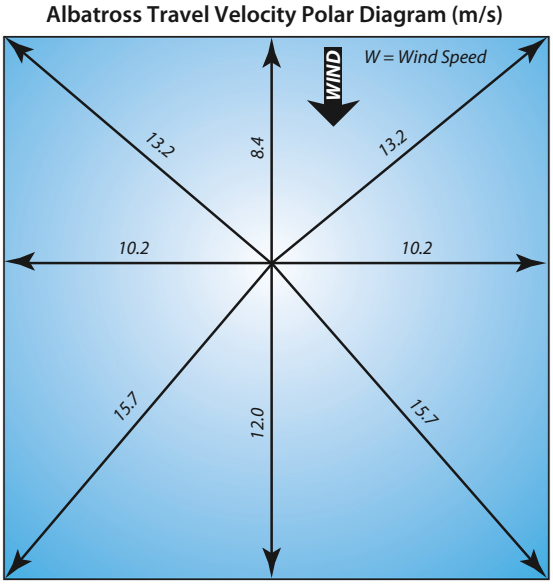

Fig. 3. Travel velocity polar diagram of a wandering albatross created using upwind and across-wind dynamic soaring modes (see Fig. 2). The square shape is a result of the equal travel velocities through the air in the along-wind and across-wind directions. Values of mean travel velocities over the ground have been added to characteristic flight directions. The diagram was created using the cruise airspeed (16.0 m/s) of the bird and the minimum wind speed (3.6 m/s) necessary for continuous dynamic soaring. Values were corrected for leeway (1.8 m/s), which was estimated to be one half of the wind speed, based on assuming that the bird spends equal time in the upper and lower layers.

wind. As a bird soars in the upper layer on a heading of 90° with respect to the wind direction (considered to come from zero degrees), for example, the wind causes a downwind leeway to the bird's right at the wind speed (3.6 m/s), so that the direction of flight over the ground is toward 103°. When descending on a 90° heading across the wind-shear layer, the apparent wind encountered by the bird shifts from straight ahead in the upper layer to the right by around 13° in the lower layer to match the bird's ground velocity toward 103°. At this point the bird could quickly yaw to the right to head straight into the apparent wind direction then bank left to start the "90°" upwind turn, which would be approximately 103°. In order to retain the upwind travel mode Raleigh cycle of approximately two 90° turns that sum to 180° a bird could descend across the wind shear layer when headed toward 83.5° (after a 83.5° turn), then quickly yaw right toward 96.5° (the direction of the bird's velocity over the ground), then bank left and turn 96.5° to head into the wind. The sum of these two turns is 180°. Presumably, a bird would know how to maximize its upwind velocity by optimally adjusting the turns somewhat like the maneuver envisioned here.

Dynamic soaring in higher wind speeds

In principle, albatrosses can use winds faster than the minimum required for dynamic soaring (3.6 m/s) to gain more energy from the wind and fly faster than the cruise airspeed of 16 m/s. They probably actually do this at least for moderate increases of airspeed. The albatross I saw using the upwind soaring mode in a wind of 7 m/s was completing the two 90° turns in around 10 s. Using these values the Rayleigh cycle model predicts that the bird could soar with an average airspeed of around 24 m/s, an average bank angle of 38°, and average acceleration of around 1.3 *g*, which seem reasonable. This airspeed corresponds to upwind and across-wind travel velocities through the air of 15.6 m/s. Correcting for leeway gives an upwind travel velocity over the ground of 12.1 m/s.

The 12.1 m/s value is almost twice as fast as the upwind travel velocity (6.7 m/s) modeled with the 16 m/s airspeed and 7 m/s wind speed. This result suggests that the albatross I observed had more than enough upwind velocity to catch up with our ship from astern as observed. The implication is that as long as the acceleration of an albatross can be kept to a reasonable level below the maximum strength of the bird's wings, the bird could increase its upwind and across-wind travel velocity with winds faster than 3.6 m/s. The Rayleigh cycle model indicates that an albatross could increase its airspeed as wind speed increases and, by increasing the period of the maneuver, maintain a constant average bank angle (45°, say) and acceleration (1.4 *g*) typical of dynamic soaring at the minimum wind speed (3.6 m/s). This suggests that the travel velocities in Table 1 and in Fig. 3 could underestimate real albatross travel velocities in wind speeds faster than 3.6 m/s.

This upwind velocity (12.1 m/s) agrees with some of the GPS tracking data analyzed by Wakefield et al. (2009). In particular, there is a cluster of around 6 observations of ground speeds of 10–13 m/s matching a head wind speed component of 7 m/s (their Fig. 2), corroborating my upwind flight observations and the Rayleigh model simulations. These GPS data and my observations indicate that at times albatrosses are quite capable of exploiting fast wind speeds in order to soar significantly faster than the typical cruise airspeed and in an upwind direction.

Comparison of the model polar diagram (Fig. 3) with Wakefield's polar diagrams

The average ground speed of wandering albatrosses is 11.8 m/s based on the travel velocity polar diagram shown in Fig. 3. This value is almost exactly equal to the 11.9 m/s average ground speed of tracked wandering albatrosses determined by Wakefield et al. (2009), as given in their Table 3. However, the square shape of the model polar differs from the rounder version provided by Wakefield and one generated using the tracking data he made available to me. Some particularly fast measured ground speeds appear to be clustered in the diagonal upwind and downwind directions, generally agreeing with the diagonal speeds in the square model polar diagram (Fig. 3). In order to investigate this issue, further analysis of the ground velocities and corresponding winds velocities will be used to document the extent to which albatrosses are able to increase their airspeed with increasing wind speed and thereby soar faster upwind as indicated by the tracking data.

The albatross tracking data used by Wakefield et al. (2009) consist of fairly infrequent GPS positions without information about the fine-scale details of the dynamic soaring flight such as high-resolution trajectories over the ground and the times to fly the various maneuvers. This kind of information is needed in order to be able to further evaluate how albatrosses use the wind to gain energy in soaring over the ocean and how fast they can fly using the different travel modes. A few albatrosses have now been tracked with higher temporal resolution GPS positions (Weimerskirch et al., 2002; Sachs et al., 2013; Bower, personal communication; see also Spivey et al., 2014). More of these high temporal resolution data including air speed measurements are needed to reveal in detail how an albatross uses dynamic soaring and to accurately model the soaring techniques.

Possible upwind dynamic soaring of a robotic albatross UAV

Recent observations of very fast radio-controlled gliders using dynamic soaring near mountain ridges suggest that these gliders

Please cite this article in press as: Richardson, P.L. Upwind dynamic soaring of albatrosses and UAVs. Prog. Oceanogr. (2014), http://dx.doi.org/10.1016/j.pocean.2014.11.002

might form the basis of a robotic albatross UAV (Unmanned Aerial Vehicle) that could use dynamic soaring to fly over the ocean faster than a real albatross. The goal of this part of the paper is to explore this concept using the observed albatross soaring modes (Fig. 4).

It should be cautioned that there are several major differences between soaring over mountain ridges and over ocean waves, and these differences raise questions about how fast a UAV could actually soar over ocean waves. Specifically, ocean waves are much smaller than mountain ridges, and this requires a UAV to fly dangerously close to the ocean surface in efficient dynamic soaring. Ocean wave fields are usually complicated and change rapidly compared to a stationary mountain ridge. Albatrosses are expert at exploiting wind–wave interactions and seem to effortlessly pick out successful dynamic soaring trajectories through complicated wave fields. Designing an auto pilot to duplicate this feat with a UAV will be a challenge. It seems clear that a robotic albatross UAV would not be able to soar over ocean waves as fast as it could over a mountain ridge. This should be kept in mind because the following discusses simulations of the maximum possible travel velocities that could be obtained using a high-performance glider in ideal conditions similar to wind blowing over a ridge.

Observations of fast dynamic soaring radio-controlled gliders

Pilots of radio-controlled gliders have used dynamic soaring to exploit winds over mountain ridges to fly gliders at astonishingly fast speeds in nearly circular loops similar to the hover mode shown in Fig. 1. In 2012 I observed gliders being flown at speeds up to around 200 m/s at Weldon Hill near Lake Isabella, California in wind speed gusts of 20–30 m/s at a height of 2.4 m above the top of the ridge. The present unofficial world record is a peak speed of 223 m/s (498 mph) held by Spencer Lisenby flying a Kinetic 100 DP glider with a 2.5 m wingspan, similar to some albatrosses (http://www.rcspeeds.com/aircraftspeeds.aspx). One almost has to see and hear these extremely fast gliders to believe how fast they can go and to appreciate their extreme performance. Anecdotal information suggests that peak glider speeds as measured by radar guns are roughly equal to 10 times the airspeed blowing over the crest of the ridge (Lisenby, personal communication).

Model simulations of fast radio-controlled gliders and possible UAVs

In order to better understand the dynamic soaring of these gliders I used the Raleigh cycle model to simulate their flight. The Rayleigh cycle model is appropriate for this because the low-wind region downwind of the mountain ridges and the fast wind speeds located just above the crest of the ridge match the two model layers. A maximum lift to drag ratio of 30/1 at a cruise speed of 25 m/s was estimated for a Kinetic 100 DP glider (Lisenby, personal communication).

Using these values the Rayleigh cycle model predicts that the maximum possible airspeed is equal to around 9.5 times the wind speed in the upper layer for wind speeds greater than around 5 m/s (Eq. (A10)). The 9.5 factor agrees quite closely with the anecdotal factor of around 10. These fast gliders need to be very strong since peak accelerations estimated from the Rayleigh cycle model and some accelerometer observations (Chris Bosley, personal communication) are around 100 g's. The gliders are highly maneuverable as demonstrated by successful dynamic soaring at high speeds close to the ground in gusty winds, by numerous remarkable acrobatic tricks, and by safely landing on top of a very windy gusty ridge. (See Richardson, 2012 for more discussion about high-speed dynamic soaring gliders.)

Fig. 4. Conceptual illustration of a robotic albatross UAV dynamic soaring over the ocean. A photo of a Kinetic 100DP glider flown by Spencer Lisenby at Weldon Hill, California was superimposed onto a photo of a black-browed albatross soaring over the Southern Ocean. Photos by Phil Richardson.

Upwind travel velocities of a robotic albatross UAV

The maximum possible upwind travel velocity of a UAV was modeled with the airspeed calculated using the Rayleigh cycle model optimized for fast flight and the upwind flight mode shown in Fig. 2. Values of maximum travel velocity through the air as a function of wind speed (W) are given in Table 1, and maximum possible upwind travel velocities over the ground as a function of wind speed given in Fig. 5. The range of possible upwind velocities plotted against wind speed is indicated in Fig. 5 by darker blue shading. An important result is the large region of possible upwind travel velocities and wind speeds for a dynamic soaring UAV.

As a numerical example, a wind speed of 10 m/s could in principle provide sufficient energy to soar at airspeeds up to 95 m/s (Eq. (A10)). The resulting maximum upwind travel velocity through the air would be 61 m/s, and the maximum diagonal travel velocity would be 86 m/s (Table 1). Correcting for leeway gives a maximum upwind velocity over the ground of 56 m/s and a maximum upwind diagonal velocity of 83 m/s. The values of the maximum possible travel velocities are illustrated in a velocity polar diagram for a UAV (Fig. 6).

Possible UAV survey mode

A main result of these calculations is to show that in principle fast upwind UAV travel velocities are possible over the ocean when using the energy extracted from the wind in dynamic soaring. In a 7 m/s wind the maximum UAV diagonal upwind travel velocity over the ground would be 58 m/s, around three times faster than that of a wandering albatross. These results indicate that the fastest way to survey or search a particular part of the ocean using a dynamic soaring UAV would be along diagonal lines (Fig. 7).

A hypothetical survey mode using diagonal lines is shown in Fig. 7. In principle a UAV could complete such a survey more than 14 times faster than a 6 m/s ship. This suggests that UAVs could provide rapid measurements over the ocean and supplement the much slower insitu sampling by ship. In addition UAVs could be used in combination with surface drifters to follow oil spills or other pollutants in the surface layer and for search and rescue operations (for example).

Discussion of UAV dynamic soaring over the ocean

The results of the Rayleigh cycle simulations indicate that much faster UAV upwind velocities are possible than those of an albatross. How much faster needs to be determined from further studies. The modeled upwind UAV travel velocities are based on the

Please cite this article in press as: Richardson, P.L. Upwind dynamic soaring of albatrosses and UAVs. Prog. Oceanogr. (2014), http://dx.doi.org/10.1016/j.pocean.2014.11.002

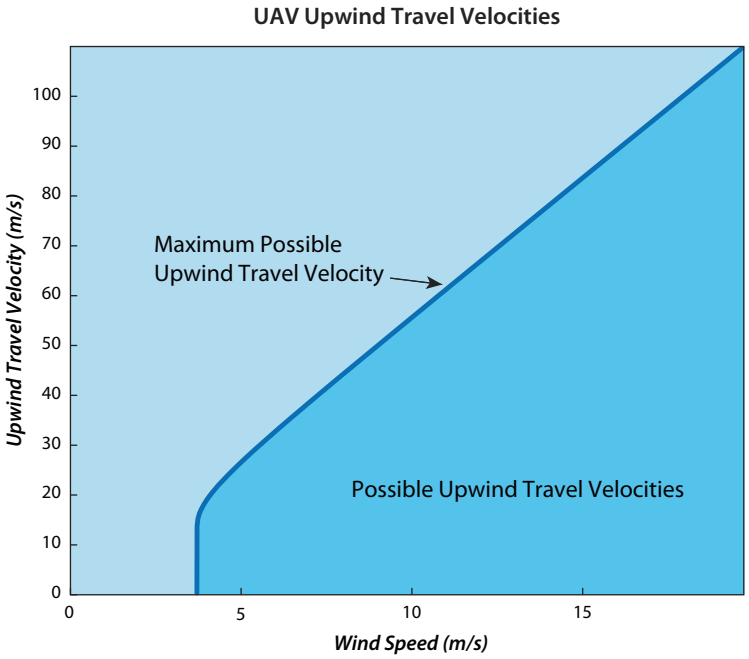

Fig. 5. Envelope of maximum possible upwind UAV travel velocities over the ground (corrected for leeway) plotted as a function of wind speed. Velocities were calculated using the upwind mode of the Rayleigh cycle model and by assuming a maximum lift/drag ratio of 30/1 at a cruise speed of 25 m/s (similar to a Kinetic 100 DP glider). The darker blue area indicates all possible upwind UAV travel velocities as a function of wind speed (W). The UAV was assumed to be able to obtain the correct amount of energy for each wind speed in order to soar upwind at slower airspeeds than the maximum possible. The simulation agree with speeds obtained by radio-controlled gliders flying over mountain ridges. The maximum possible speeds are probably significantly faster than those possible by a UAV soaring over the ocean like an albatross. (For interpretation of the references to colour in this figure legend, the reader is referred to the web version of this article.)

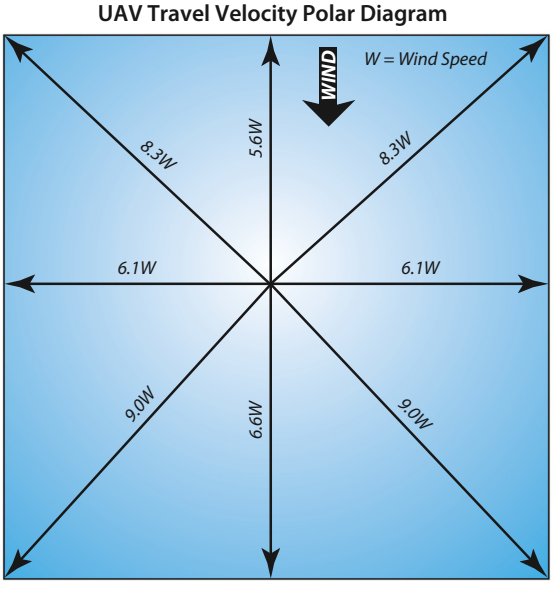

Fig. 6. Travel velocity polar diagram of a robotic albatross UAV. The square shape is a result of the equal travel velocities through the air in the along-wind and across-wind directions. The diagram was created by assuming a characteristic lift/drag ratio of 30/1, a cruise velocity of 25 m/s (similar to a Kinetic 100 DP glider), and by calculating airspeeds based on the Raleigh cycle model optimized to give the maximum possible airspeed for a given wind speed. Travel velocities have been corrected for leeway and represent velocities over the ground. Specific given values of travel velocity represent the linear relation between travel velocity over the ground and wind speed (W) for wind speeds over around 5 m/s (see text). For example, a wind speed of 10 m/s results in maximum possible travel velocities over the ground of 56 m/s upwind, 83 m/s diagonally upwind, and 61 m/s across-wind. Because of the differences between dynamic soaring over a mountain ridge and over ocean waves, these plotted speeds are probably significantly larger than those obtainable by a UAV soaring over the ocean like an albatross.

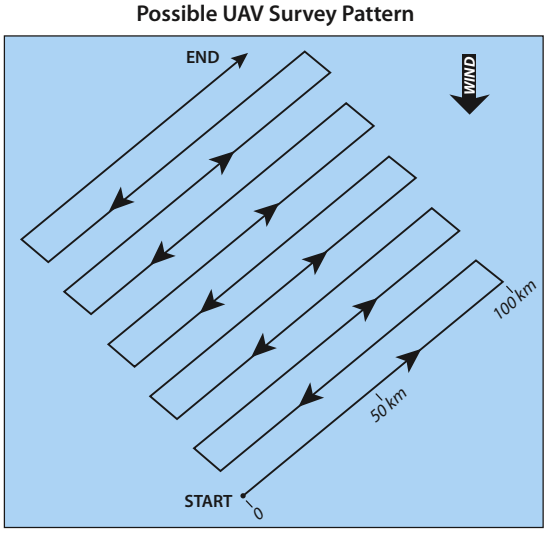

Fig. 7. Schematic diagram showing a possible UAV survey mode using a combination of upwind and downwind modes of the Rayleigh cycle consisting of diagonal trajectories with respect to the wind direction (Fig. 2). Diagonal velocities are the fastest possible travel velocities over the ocean using the upwind (and downwind) mode. They enable rapid surveying of an area for any given wind direction given sufficient wind for dynamic soaring. For example, in a wind speed of 10 m/s the average maximum possible diagonal velocities are around 86 m/s (Fig. 6). This speed is probably significantly faster than what could be achieved in practice by a UAV soaring over ocean waves.

observed albatross dynamic soaring flight patterns. A fundamental question is how well can a UAV mimic albatross maneuvers and also increase the frequency of shear-layer crossings in order to gain sufficient energy for fast travel velocities?

Please cite this article in press as: Richardson, P.L. Upwind dynamic soaring of albatrosses and UAVs. Prog. Oceanogr. (2014), http://dx.doi.org/10.1016/j.pocean.2014.11.002

In the low-level part of a swoop in a wave trough, an albatross flies very close to the ocean surface, close enough so that the bird's wing tip often grazes the surface. This allows the bird to descend into a lee eddy located in a wave trough and be shielded from the full force of the wind. Grazing the water surface with wing tip feathers is not a problem for an albatross, but touching the wing of a UAV could cause a crash. Thus, a UAV must maintain a safe gliding distance above the ocean surface. But, to fully exploit gust soaring a UAV must be able to descend below the wind-shear layer into a wave trough, and this could be compromised if the minimum safe flying height above the ocean surface were greater than the wave height. Therefore, it seems likely that increasing a UAV's height above the ocean for safety could reduce energy gained from the available wind shear, especially in low-amplitude waves. As demonstrated by the numerical simulations of dynamic soaring over a flat ocean, crossing only part of the main wind-shear layer limits the energy gain, airspeed, and upwind travel velocity of a UAV.

Clearly, there is a wide range of possible UAV upwind travel velocities using dynamic soaring as indicated in Fig. 5. It is necessary to establish values optimized for flight over real ocean waves in various wind conditions and to refine such a figure. To do so it would be beneficial to have experienced pilots of RC gliders take various waterproof gliders to sea and experiment with field trials in order to measure how fast dynamic soaring could be accomplished in realistic winds and waves. In such trials it would be helpful to have the gliders instrumented to measure high temporal resolution series of positions, orientations, accelerations and velocities through the air as well as observations of the wind and waves.

Design of a robotic albatross UAV

The UAV discussed here was modeled on the kinetic 100 DP high-performance glider (large maximum lift/drag ~30, large cruise airspeed ~25 m/s), which is optimized for fast dynamic soaring using fast winds blowing over mountain ridges and not optimized for slower winds blowing over waves like albatrosses often exploit. An appropriate robotic albatross UAV should probably be optimized for slower winds, which can often limit dynamic soaring over the ocean, perhaps having a performance similar to a wandering albatross (maximum lift/drag ~21, cruise airspeed ~16 m/s). In very slow winds some albatrosses often use a flap-gliding technique to supplement dynamic soaring, and they also exploit updrafts over waves. When the wind dies altogether the birds typically land on the water. A useful UAV would also need auxiliary power for slow winds and, perhaps, the ability to land on water and take off again. Because of drag, these features would tend to reduce UAV's airspeeds. Other important developments are sensors to measure winds and waves from a UAV and an autopilot that could implement dynamic soaring using these measurements.

Summary of results

An upwind dynamic soaring mode was modeled using a series of 90° turns linking upwind climbs across the wind-shear layer and across-wind descents across the wind-shear layer (Fig. 2). A similar downwind mode can be used to soar by descending downwind across the wind-shear layer instead of climbing upwind across it. A series of 90° turns can be combined to soar in any direction including directly upwind and downwind somewhat similar to the courses made good by a sailboat tacking in the wind (Fig. 2).

A travel velocity polar diagram was constructed for wandering albatrosses by combining the upwind and across-wind travel modes using the 3.6 m/s minimum wind speed for energy-neutral dynamic soaring (Fig. 3). The upwind component of travel velocity over the ground is 8.4 m/s, considerably larger than the minimum wind speed (3.6 m/s). The fastest travel velocity over the ground in the upwind half of the diagram is 13.2 m/s along diagonals heading in a direction of around 51° relative to the wind direction. The Rayleigh cycle model was also used to simulate how an albatross could increase its airspeed using faster winds than 3.6 m/s and soar significantly faster upwind similar to the speeds of some wandering albatrosses tracked by GPS. In particular, the upwind travel velocity of an albatross soaring in a wind of 7 m/s was calculated to be around 12 m/s, more than enough to explain how the bird was able to catch up to our ship that was steaming upwind at 6 m/s into a 7 m/s head wind.

The concept of a fast dynamic soaring robotic albatross UAV was explored based on the characteristics of high speed radio-controlled gliders, which have exploited dynamic soaring to reach speeds up to 220 m/s. Maximum possible airspeeds of a such a UAV were simulated by optimizing the Rayleigh cycle model for maximum airspeed. Although such fast airspeeds might not be achievable in practice by a UAV soaring over the ocean for reasons mentioned above, the speeds and resulting travel velocities give an indication of the maximum possible using the Rayleigh cycle. The wide range of possible UAV upwind travel velocities as a function of wind speed was shown in Fig. 5.

A polar diagram of UAV travel velocities over the ground as a function of wind speed is given in Fig. 6. The maximum possible upwind travel velocity in a 10 m/s wind was found to be 56 m/s and the maximum diagonal upwind velocity is 83 m/s. These very fast speeds demonstrate the power of using dynamic soaring and suggest that in principle UAV travel velocities over the ocean could be much faster than that of albatrosses. It remains for further studies to demonstrate how fast a UAV can soar over the ocean. Fig. 5 also indicates that a dynamic soaring UAV could travel in any direction over the ocean and not be limited by the small upwind travel velocities predicted by some models that include a flat ocean. The fast diagonal travel velocities suggest that a rapid search or survey mode over the ocean might consist of a series of parallel diagonal tracks relative to the wind direction offset from each other as illustrated in Fig. 7.

Conclusions and recommendations

The results of this study suggest that a robotic albatross UAV could soar much faster than an albatross and be useful for many applications. In order to evaluate how effectively an AUV could soar over the real ocean in different wind and wave condition several studies could to be undertaken. First, numerical simulations could be made of the interaction of winds and waves, of the resulting structures in the wind field including updrafts and detached shear layers, and of the optimal dynamic soaring patterns using the wind field over ocean waves. Second, albatrosses could be instrumented to better measure their dynamic soaring techniques in various winds and waves. Specifically, high temporal resolution time series could be obtained of albatrosses' positions, velocities, orientations, accelerations, and airspeeds, and these related to in situ observations of winds and waves. Third, expert pilots of radio-controlled gliders who are experienced in fast dynamic soaring could conduct field tests in order to evaluate fast dynamic soaring over the ocean with various waterproof gliders and to establish safe minimum soaring heights above the ocean surface. These gliders should be instrumented as would be the albatrosses mentioned above. Using the results of the simulations and measurements of albatross and radio-controlled glider flight, a dynamic soaring autopilot could be developed. Finally, a prototype waterproof, instrumented, dynamic soaring UAV with backup auxiliary power could be constructed and tested over the ocean.

Please cite this article in press as: Richardson, P.L. Upwind dynamic soaring of albatrosses and UAVs. Prog. Oceanogr. (2014), http://dx.doi.org/10.1016/j.pocean.2014.11.002

Acknowledgements

This paper was stimulated by the observed flight of albatrosses and radio-controlled gliders and by discussions of dynamic soaring with Peter Lissaman and Colin Taylor. Financial support was provided by the F. Livermore Trust and Woods Hole Oceanographic Institution emeritus funds. Paul Oberlander prepared the figures. Two anonymous reviewers provided helpful critical comments on an earlier version of this paper.

Appendix A

Nomenclature

C_l	lift coefficient
C_d	drag coefficient
d	diameter of loop
d_{opt}	Optimum diameter of loop for maximum airspeed
D	Drag force
g	Gravity
L	Lift force
m	Mass
t	Period of loop (or equivalent sum of angles turned)
t_{opt}	Optimum loop period for maximum airspeed
S	Characteristic wing area
V	Airspeed of albatross or UAV
V_c	Cruise airspeed at maximum glide ratio $(V/V_z)_{\max}$
V_z	Sink rate due to drag
ΔV	Increase of airspeed caused by crossing the wind-shear layer
W	Wind speed of upper layer
ΔW	Increase of wind speed across the wind-shear layer
φ	Bank angle
ρ	Density of air

Rayleigh cycle model

In the Rayleigh cycle model the sudden gain in airspeed of a glider climbing across the wind-shear layer headed into the wind is ΔV. This ΔV is assumed to equal the vertical increase of wind speed (ΔW) across the layer and also the wind speed W of the upper layer, assuming zero wind speed in the lower layer. A similar increase of airspeed is obtained by a glider descending across the wind-shear layer headed downwind.

The sink rate V_z of a glider at constant airspeed was used to obtain the decrease of airspeed at constant height as modeled by the Rayleigh cycle. To do this the rate of change of kinetic energy, $d/dt(mV^2/2) = mV(dV/dt)$, at constant height was equated to the rate of change of potential energy, $d/dt(mgh) = mgV_z$, at constant airspeed. The result indicates that $dV/dt = g/(V/V_z)$, where V/V_z represents values of the glide ratio (glide polar). Values of the glide ratio are closely equal to values of lift/drag (L/D) for L/D values $\gg 1$ typical of glider flight. Lift $L = Cl(\rho/2)V^2S$ and drag $D = Cd(\rho/2)V^2S$.

V/V_z is nearly constant in the relevant glider airspeed range ΔV centered a particular average airspeed, and therefore acceleration is nearly constant and airspeed decreases nearly linearly in time due to drag. For example, values of V/V_z are within around 1% of the mean V/V_z in the energy-neutral circle of a wandering albatross soaring with a cruise airspeed of 16 m/s. Thus, the total decrease of airspeed ΔV in a half loop ($t/2$) is given by

$$\Delta V = \frac{gt}{2(V/V_z)}, \tag{A1}$$

Values of V/V_z were modeled using the aerodynamic equations of motion for balanced circular flight (Lissaman, 2005; Torenbeek and Wittenberg, 2009) and a quadratic drag law, in which the drag coefficient is proportional to the lift coefficient squared. In balanced circular flight the horizontal component of lift balances the centripetal acceleration and the vertical component of lift balances gravity. Specifically, V/V_z was modeled by

$$V/V_z = \frac{2(V/V_z)_{\max}}{(V/V_c)^2 + (V_c/V\cos\varphi)^2}, \tag{A2}$$

where $(V/V_z)_{\max}$ is the maximum glide ratio at V_c the associated cruise airspeed (airspeed of minimum drag) of a representative glider in straight flight, φ is the bank angle, and $\cos\varphi$ is given by

$$\cos\varphi = \sqrt{\frac{1}{(2\pi V/gt)^2 + 1}}. \tag{A3}$$

Combining Eqs. (A2) and (A3) with (A1) and assuming that $\Delta V = W$ indicates that

$$\Delta V = W = \frac{gt}{4(V/Vz)_{\max}}[(V/V_c)^2 + (V_c/V)^2 + (2\pi V_c/gt)^2] \tag{A4}$$

The $(2\pi V_c/gt)^2$ term is due to the centripetal acceleration and bank angle. Eq. (A4) indicates that for a particular glider (with a given $(V/V_z)_{\max}$ at V_c) in energy-neutral soaring, the increase of glider airspeed (ΔV) gained by crossing the wind-shear layer and the gradual loss in a half loop is a function of both the loop period t and the average airspeed V.

A minimum ΔV (and minimum W) for a given glider airspeed occurs at an "optimum" loop period t_{opt} coinciding with minimum energy loss in a loop (minimum $V_z t$). The optimum loop period (t_{opt}) was obtained by setting the derivative $d(\Delta V)/dt$ of (Eq. (A4)) equal to zero and solving for t.

$$t_{opt} = \frac{2\pi V_c/g}{\sqrt{(V/V_c)^2 + (V_c/V)^2}}. \tag{A5}$$

Eq. (A5) indicates that t_{opt} decreases with increasingly large V. In sufficient wind flight faster than the cruise airspeed V_c can be accomplished by decreasing the loop period toward t_{opt} and increasing the frequency of shear-layer crossings. Substituting Eq. (A5) into Eq. (A4) provides an expression for minimum ΔV (and minimum W) for a given V. Thus the minimum wind speed $W_{\min}$ needed for a given glider airspeed V in energy neutral dynamic soaring is given by

$$W_{\min} = \frac{\pi V_c}{(V/V_z)_{\max}}\sqrt{(V/V_c)^2 + (V_c/V)^2} \tag{A6}$$

This equation can be used to calculate the maximum possible airspeed $V_{\max}$ for a given wind speed W. Eq. (A6) indicates that the absolute minimum $W_{\min}$ occurs when $V = V_c$, and thus the equation for the absolute minimum $W_{\min}$ is

$$W_{\min} = \frac{\pi V_c\sqrt{2}}{(V/V_z)_{\max}}. \tag{A7}$$

At fast glider speeds >50 m/s and for $V_c \sim 25$ m/s, $(V/V_c)^2 \gg (V_c/V)^2$ and $(V_c/V)^2$ can be neglected. This simplifies Eq. (A5) to

$$t_{opt} = \frac{2\pi V_c^2}{gV}. \tag{A8}$$

Substituting Eq. (A8) into Eq. (A4) provides a simplified expression for minimum ΔV (and minimum W) for $V > 50$ m/s. Thus the minimum wind speed $W_{\min}$ needed for a given glider airspeed $V > 50$ m/s in energy neutral dynamic soaring is given by

$$W_{\min} = \frac{\pi}{(V/V_z)_{\max}}(V). \quad \text{(A9)}$$

This equation can be rearranged to provide the maximum glider airspeed $V_{\max}$ for a given wind speed W

$$V_{\max} = \frac{(V/V_z)_{\max}}{\pi}(W). \quad \text{(A10)}$$

Eq. (A10) indicates that for fast flight (>50 m/s) the maximum possible (average) airspeed in a Rayleigh cycle is proportional to wind speed. It is important to note that this linear relation depends on flying with an optimum loop period. Other loop periods can result in a smaller maximum airspeed for a given wind speed. Maximum lift/drag ratio $(L/D)_{\max}$ is approximately equal to the maximum glide polar $(V/V_z)_{\max}$ and can be substituted into the above equations. Thus the maximum possible average airspeed of a dynamic soaring glider is proportional to its maximum lift/drag.

The diameter of a loop is given by $d = Vt/\pi$. Substituting into this equation the expression for optimum loop period t_{opt} in fast flight (Eq. (A8)) gives the optimum loop diameter d_{opt}

$$d_{opt} = 2V_c^2/g. \quad \text{(A11)}$$

Eq. (A11) reveals that for fast flight the optimum loop diameter is proportional to cruise airspeed squared but is independent of glider airspeed.

The total acceleration of a glider includes centripetal acceleration and gravity and is given by the load factor, which equals $1/\cos\varphi$ (see Eq. (A3)). For fast dynamic soaring, $V > 50$ m/s, $(2\pi V/gt)^2 \gg 1$, and the load factor is approximately equal to $2\pi V/gt$.

References

Alerstam, T., Gudmundsson, G.A., Larsson, B., 1993. Flight tracks and speeds of Antarctic and Atlantic seabirds: radar and optical measurements. Philosophical Transactions of the Royal Society of London B 340, 55–67.

Baines, A.C., 1889. The sailing flight of the albatross. Nature 40, 9–10.

Barnes, J.P., 2004. How Flies the Albatross—the Flight Mechanics of Dynamic Soaring, 2004. SAE Technical Paper 2004-01-3088, p. 18.

Bower, G.C., 2012. Boundary layer dynamic soaring for autonomous aircraft: design and validation. Ph.D. dissertation, Department of Aeronautics and Astronautics, Stanford University, unpublished.

Deittert, M., Richards, A., Toomer, C.A., Pipe, A., 2009. Engineless UAV propulsion by dynamic soaring. Journal of Guidance, Control, and Dynamics 2 (5), 1446–1457.

Gent, P.R., Taylor, P.A., 1977. A note on "separation" over short wind waves. Boundary-Layer Meteorology 11, 65–87.

Hristov, T.S., Miller, S.D., Friehe, C.A., 2003. Dynamical coupling of wind and ocean waves through wave-induced air flow. Nature 422, 55–58.

Hsu, C.-T., Hsu, E.Y., Street, R.L., 1981. On the structure of turbulent flow over a progressive water wave: theory and experiment in a transformed, wave-following co-ordinate system. Journal of Fluid Mechanics 105, 87–117.

Idrac, P., 1925. Étude expérimentale et analytique du vol sans battements des oiseaux voiliers des mers australes, de l'Albatros en particulier. La Technique Aeronautique 16, 9–22.

Lissaman, P., 2005. Wind energy extraction by birds and flight vehicles. American Institute of Aeronautics and Astronautics Paper 2005-241, January 2005, p. 13.

Pennycuick, C.J., 1982. The flight of petrels and albatrosses (Procellariiformes), observed in South Georgia and its vicinity. Philosophical Transactions of the Royal Society of London B 300, 75–106.

Pennycuick, C.J., 2002. Gust soaring as a basis for the flight of petrels and albatrosses (Procellariiformes). Avian Science 2, 1–12.

Pennycuick, C.J., 2008. Modelling the Flying Bird. Academic Press, New York, p. 496.

Rayleigh, J.W.S., 1883. The soaring of birds. Nature 27, 534–535.

Reul, N., Branger, H., Giovanangeli, J.-P., 1999. Air flow separation over unsteady breaking waves. Physics of Fluids 11 (7), 1959–1961.

Richardson, P.L., 2011. How do albatrosses fly around the world without flapping their wings? Progress in Oceanography 88, 46–58.

Richardson, P.L., 2012. High-speed dynamic soaring. Radio-Controlled Soaring Digest 29 (4), 36–49.

Sachs, G., 2005. Minimum shear wind strength required for dynamic soaring of albatrosses. Ibis 147, 1–10.

Sachs, G., Traugott, J., Nesterova, A.P., Bonadonna, F., 2013. Experimental verification of dynamic soaring in albatrosses. Journal of Experimental Biology 216, 4222–4232.

Spivey, R.J., Stansfield, S., Bishop, C.M., 2014. Analysing the intermittent flapping flight of a Manx Shearwater, *Puffinus puffinus*, and its sporadic use of a wave-meandering wing-sailing flight strategy. Progress in Oceanography 125, 62–73.

Sullivan, P.P., McWilliams, J.C., Moeng, C.-H., 2000. Simulations of turbulent flow over idealized water waves. Journal of Fluid Mechanics 404, 47–85.

Torenbeek, E., Wittenberg, H., 2009. Flight Physics: Essentials of Aeronautical Disciplines and Technology, with Historical Notes. Springer, New York, p. 535.

Wakefield, E.D., Phillips, R.A., Matthiopoulos, J., Fukuda, A., Higuchi, H., Marshall, G.J., Trathan, P.N., 2009. Wind field and sex constrain the flight speeds of central-place foraging albatrosses. Ecological Monographs 79, 663–679.

Weimerskirch, H., Guionnet, T., Martin, J., Shaffer, S.A., Costa, D.P., 2000. Fast and fuel efficient? optimal use of wind by flying albatrosses. Proceedings of the Royal Society of London B 267, 1869–1874.

Weimerskirch, H., Bonadonna, F., Bailleul, F., Mabille, G., Dell'Omo, G., Lipp, H.-P., 2002. GPS tracking of foraging albatrosses. Science 295, 1259.

Please cite this article in press as: Richardson, P.L. Upwind dynamic soaring of albatrosses and UAVs. Prog. Oceanogr. (2014), http://dx.doi.org/10.1016/j.pocean.2014.11.002